

Ex Vivo and in Vivo Effects of Isfagomine on Acid β -Glucosidase Variants and Substrate Levels in Gaucher Disease*

Received for publication, July 6, 2011, and in revised form, December 8, 2011. Published, JBC Papers in Press, December 14, 2011, DOI 10.1074/jbc.M111.280016

Ying Sun^{†§}, Benjamin Liou[‡], You-Hai Xu^{†§}, Brian Quinn[‡], Wujuan Zhang[¶], Rick Hamler^{||}, Kenneth D. R. Setchell^{§¶}, and Gregory A. Grabowski^{†§¶1}

From the Divisions of [‡]Human Genetics and [¶]Pathology and Laboratory Medicine, Cincinnati Children's Hospital Medical Center and the [§]Department of Pediatrics, University of Cincinnati College of Medicine, Cincinnati, Ohio 45229-3039 and ^{||}Amicus Therapeutics Inc., Cranbury, New Jersey 08512

Background: "Chaperones" may enhance mutant enzyme activities, but therapeutic levels have not been shown *in vivo*.

Results: A chaperone, isfagomine, stabilizes wild type and mutant acid β -glucosidases in tissues and sera and reduces visceral substrates *in vivo*.

Conclusion: These effects are enhanced pre- versus postsynthetically.

Significance: The results are proof of principle for the potential therapeutic use in residual enzyme diseases.

Isfagomine (IFG) is an acid β -glucosidase (GCase) active site inhibitor that acts as a pharmacological chaperone. The effect of IFG on GCase function was investigated in GCase mutant fibroblasts and mouse models. IFG inhibits GCase with $K_i \sim 30$ nM for wild-type and mutant enzymes (N370S and V394L). Fibroblasts treated with IFG at μ M concentrations showed enhancement of WT and mutant GCase activities and protein levels. Administration of IFG (30 mg/kg/day) to the mice homozygous for GCase mutations (V394L, D409H, or D409V) led to increased GCase activity in visceral tissues and brain extracts. IFG effects on GCase stability and substrate levels were evaluated in a mouse model (hG/4L/PS-NA) that has doxycycline-controlled human WT GCase (hGCase) expression driven by a liver-specific promoter and is also homozygous for the IFG-responsive V394L GCase. Both human and mouse GCase activity and protein levels were increased in IFG-treated mice. The liver-secreted hGCase in serum was stabilized, and its effect on the lung and spleen involvement was enhanced by IFG treatment. In 8-week IFG-treated mice, the accumulated glucosylceramide and glucosylsphingosine were reduced by 75 and 33%, respectively. Decreases of storage cells were correlated with >50% reductions in substrate levels. These results indicate that IFG stabilizes GCase in tissues and serum and can reduce visceral substrates *in vivo*.

Mutations of the acid β -glucosidase gene (*GBA1*) lead to a common inherited lysosomal storage disease, Gaucher disease, that results from defects in the degradation by acid β -glucosidase (GCase)² of substrates glucosylceramide (GC) and gluco-

sylysphingosine (GS). Depending on the organ involvement, Gaucher disease is classified into three types. Type 1 is a visceral disease manifested by hepatosplenomegaly and hematologic and skeletal dysfunction (1), type 2 is an acute neuronopathic disease, and type 3 is a subacute neuronal/visceral disease. Over 350 mutations have been identified in affected patients (1, 2). Some of the mutations are caused by recombination between *GBA1* and pseudogene (3), which creates difficulties in assessments of genotype and phenotype correlation in Gaucher disease. The accumulation of the substrates leads to enlargement of the liver and spleen, bone lesions, and central nervous system manifestations (1, 4, 5). The macrophage is the primary cell displaying substrate accumulation (1).

Of the disease-causing mutations in *GBA1*, many are rare or occur in single families (1). Homozygosity for N370S is associated with type 1, non-neuronopathic disease and variable visceral involvement (1, 6, 7). The N370S mutation has high frequency in the Ashkenazi Jewish population. The L444P recurrent mutation is highly associated with neuronopathic variants of Gaucher disease and is the most common Gaucher disease allele worldwide (1). The D409H alleles also have significant frequency, and D409H homozygotes manifest early onset of variable visceral and CNS involvement (8, 9). Uniquely, calcific aortic root and valve disease occurs with D409H homozygosity (9). The V394L allele in humans has been reported only in the heteroallelic state and is associated with either type 1, 2, or 3 depending on the heteroallele and genetic background (10).

Mouse models having *Gba1* mutations have been generated. In contrast to humans, N370S or L444P (as an insertional mutant) homozygosity in mice leads to death within 24–48 h (11, 12). Homozygosity for V394L or D409H leads to defective GCase activity, but mice survive to \sim 24 months with only minor visceral abnormalities (11). More extensive involvement in such mouse models was developed by cross-breeding of V394L or D409H with a hypomorphic prosaposin-deficient

* This work was supported, in whole or in part, by National Institutes of Health Grants HD 059823, DK 36729, and NS 36681 (to G. A. G.).

¹ To whom correspondence should be addressed: Cincinnati Children's Hospital Medical Center, Division of Human Genetics, 3333 Burnet Ave., MLC 4006, Cincinnati, OH 45229-3039. Tel.: 513-636-7290; Fax: 513-636-2261; E-mail: greg.grabowski@cchmc.org.

² The abbreviations used are: GCase, acid β -glucosidase; hGCase, human WT GCase; GS, glucosylsphingosine; GC, glucosylceramide; IFG, isfagomine;

DOX, doxycycline; Bis-Tris, 2-[bis(2-hydroxyethyl)amino]-2-(hydroxymethyl)propane-1,3-diol; CRIM, cross-reacting immunological material.

Gaucher Disease Therapy

mouse, termed 4L/PS-NA or 9H/PS-NA, respectively (13). Such mice show numerous engorged macrophages and large GC accumulations. GCCase is not secreted out of cells except when heavily overexpressed (14–16). Conditional expression of human wild-type (WT) GCCase (hGCCase) in the liver of 4L/PS-NA mice (hG/4L/PS-NA) leads to secretion of the human enzyme into serum, reduction of GC tissue accumulation, and improvement in the visceral phenotype (14). The expression of hGCCase in hG/4L/PS-NA mice is driven by liver-enriched activator promoter and controlled by the tetracycline transcriptional activation system. This model provides a system to evaluate endogenous enzyme therapy for Gaucher disease and assess substrate accumulation following periods off enzyme therapy.

Two therapeutic approaches are available for treating Gaucher disease patients. Enzyme reconstitution therapy is accomplished by infusing recombinant macrophage-targeted hGCCase to supplement the residual activity of the endogenous mutant enzyme. Substrate synthesis inhibition therapy seeks to reduce substrate levels by decreasing glucosylceramide production through inhibition of glucosylceramide synthase. Additional pharmacological small molecule approaches have been proposed to treat Gaucher disease by enhancing mutant enzyme stability and trafficking to lysosomes (17, 18). Isfagomine (IFG), a competitive inhibitor, binds to the active site of GCCase with high affinity at neutral pH in endoplasmic reticulum where GCCase has decreased stability and with low affinity in the acidic lysosomes where IFG can be released from GCCase. The binding of IFG to GCCase enhances its folding, stability, and trafficking to lysosomes (19, 20). This effect has been called chaperoning; we prefer the term enzyme enhancement therapy. Several mutant GCases show increases in enzymatic activity and protein in response to IFG (19–21). IFG is distributed to brain, bone marrow, and visceral tissues following oral administration (21). The peak level of IFG in tissues reached within 1 h after administration is in the order liver > plasma > spleen > brain with half-lives of 2.6, 4.4, 4.6, and 9 h, respectively (21). However, the outcome of IFG treatment on substrate accumulation has not been reported.

Here, the effects of IFG on mutant GCases were evaluated with recombinant enzymes and in cultured fibroblasts and that displayed enzyme deficiencies (11). The effects of IFG on substrate levels were evaluated in the hG/4L/PS-NA model that has doxycycline (DOX)-controllable hGCCase expression in the liver (14).

EXPERIMENTAL PROCEDURES

Materials—The following were from commercial sources: 4-methylumbelliferyl β -D-glucopyranoside (Biosynth AG, Switzerland); sodium taurocholate (Calbiochem); mouse anti- β -actin monoclonal antibody (Sigma); NuPAGE 4–12% Bis-Tris gel, NuPAGE MES SDS running buffer, and DMEM (Invitrogen); rat anti-mouse CD68 monoclonal antibody (Serotec, Oxford, UK); M-PER Mammalian Protein Extraction Reagent and BCA Protein Assay Reagent (Pierce); HybondTM-ECLTM nitrocellulose membrane and ECL detection reagent (Amersham Biosciences); and ABC Vectastain and Alkaline Phosphatase kit II (Black) (Vector Laboratories, Burlingame, CA). IFG

tartrate was from Amicus Therapeutics Inc. (Cranbury, NJ). Imiglucerase was from Genzyme Corp. (Cambridge, MA).

Expression and Purification of GCases—The mutant *GBA1* constructs were generated from the human cDNA and cloned into pBluescript 4.5 (Invitrogen) after site-directed mutagenesis (QuikChange, Stratagene). The specific mutations and the entire clones were validated by complete DNA sequencing. The baculoviruses containing the requisite human *GBA1* cDNAs were purified and then used to express hGCases that were subsequently purified from protein-free medium (22).

Inhibitor Interactions with Mutant GCases—The GCCase activities were determined fluorometrically as described (22). The IC_{50} values for IFG with each GCCase were determined by using various concentrations of IFG that were incubated with homogeneous hGCCase (imiglucerase) or the purified human mutant GCCase (N370S or V394L) from insect cell medium. IFG was shown to be a competitive inhibitor of each GCCase variant form (22). The experiments were performed in triplicate and repeated thrice. GraphPad Prism 5 software was used for data analysis.

Cultured Skin Fibroblasts—Human fibroblast lines that contained the WT, N370S/84GG (84GG is a null mutation), and L444P/L444P GCases were obtained from the Coriell Cell Repository. Mouse fibroblast cells with the designated genotypes were established from newborn pups (11, 13). The cells were incubated for 5 days in the medium containing IFG at the indicated concentrations. The cells were washed thrice prior to harvest, and the cell pellets were resuspended in 0.25% sodium taurocholate and 0.25% Triton X-100 and lysed by cup sonication in an ice water bath for 3×1 -min cycles. The cell lysates were used for enzymatic assays and cross-reacting immunological material (CRIM) determinations.

Colocalization of GCases and Lamp1 in Fibroblast—The fibroblasts were incubated with IFG for 5 days and reseeded on the chamber slides at a density of 5000 cells/cm² in fresh medium containing IFG for an additional 2 days. The cells were then fixed in 3% paraformaldehyde in PBS (pH 7.4) at room temperature for 40 min, washed twice with PBS, and quenched with 50 mM NH₄Cl for 10 min. Following two PBS washes, the cells were incubated with 0.5% saponin in PBS (pH 7.4) for 30 min at room temperature. After two washes with PBS, the cells were treated with 1.5% nonfat dry milk, 1.5% BSA, and 0.5% gelatin in PBS and incubated with goat anti-hGCCase (1:50) and rabbit anti-human Lamp1 for human fibroblasts or with rabbit anti-mouse GCCase (1:100) and rat anti-mouse Lamp1 (1:50; Research Diagnostics Inc., MCD107A-D4B) for mouse fibroblasts. The following secondary antibodies were used for detection: horse anti-goat biotin and streptavidin-Alexa Fluor 610 (1:100; Invitrogen) S32359 for hGCCase, goat anti-rabbit FITC (1:100; ICN Biomedicals, 55664) for human Lamp1; and goat anti-rabbit FITC for mouse GCCase and donkey anti-rat Texas Red (1:100; Abcam, ab6732-1) for mouse Lamp1. Images were captured with a Zeiss Apotome microscope (AxioV200) at an excitation of 488 (for FITC) or 599 nm (for Alexa Fluor 610 and Texas Red).

Mouse Models and IFG Treatment—Mice homozygous for *Gba1* encoding V394L (4L), D409V (9V), and D409H (9H) GCases (11) and 4L/PS-NA (PS-NA;V394L/V394L) mice were

as described (13). The 4L/PS-NA mice contain a hypomorphic prosaposin cDNA against a prosaposin knock-out (PS^{-/-}) background that also had the *Gba1* encoding homozygous V394L (13). hG/4L/PS-NA mice are generated by breeding 4L/PS-NA with two transgenic lines: one containing the tetracycline transactivator driven by liver-enriched activator promoter and one having the hGCCase cDNA constructed into the vector containing a tetracycline-responsive promoter element (Tet-Off) (14). The strain backgrounds for hG/4L/PS-NA and 4L/PS-NA mice are 1/2:1/4:1/4, FVB;C57BL/6;129SvEvbrd, and those for the 4L, 9H, and 9V are 1/2:1/2, C57BL/6;129SvEvbrd. The mice were provided drinking water containing sufficient IFG to supply 30 mg/kg/day based on the assessed daily water consumption of 8 ml/day. The mice were maintained in a microisolator pathogen-free environment in accordance with institutional guidelines under Institutional Animal Care and Use Committee approval at Cincinnati Children's Hospital Research Foundation.

GCCase Activity Assays and CRIM Determinations—Tissues and cell pellets were homogenized in 0.25% sodium taurocholate and 0.25% Triton X-100. GCCase activities were determined fluorometrically with 4-methylumbelliferyl β -D-glucopyranoside as substrate (11).

CRIM for each GCCase variant in fibroblasts was determined by immunoblot with rabbit anti-human or anti-mouse GCCase polyclonal antisera assuming equal reactivity of the GCCase in variants and wild type. Aliquots containing equal GCCase activity were applied to 10% SDS gels for immunoblot analysis. The density of the band corresponding to intact GCCase CRIM was quantified in duplicate using ImageQuant 5.2 software. The known masses of homogeneous hGCCase (2.5, 5, and 10 ng) were used as a standard on each gel. Serum hGCCase activity and protein were determined (14).

Mouse tissues were homogenized in M-PER Mammalian Protein Extraction Reagent. Protein concentrations were estimated using BCA Protein Assay Reagent. Tissue extracts were separated on NuPAGE 4–12% Bis-Tris gels with NuPAGE MES SDS running buffer and electroblotted on Hybond-ECL nitrocellulose membranes. The membranes were blocked with 3% BSA in 1× PBS for 1 h followed by incubation overnight with either rabbit anti-mouse GCCase (1:2000) or anti-hGCCase (1:2000) in 1.5% BSA and 1× PBS. The goat anti-rabbit HRP (1:1500) conjugate was used to detect mouse GCCase or hGCCase. The signals were developed using ECL detection reagent according to the manufacturer's instructions. Mouse anti- β -actin monoclonal antibody (1:10,000 in 1.5% BSA) was applied to detect β -actin as a loading control. The density of the bands corresponding to GCCase and β -actin were quantified in duplicate using ImageQuant 5.2 software.

Histological Studies—For immunohistochemistry, mouse tissues were perfused with saline followed by 4% paraformaldehyde and collected. Frozen tissue sections fixed with 4% paraformaldehyde were incubated with rat anti-mouse CD68 monoclonal antibody (1:200 in PBS with 5% BSA) overnight at 4 °C. Detection was performed using ABC Vectastain and Alkaline Phosphatase kit according to the manufacturer's instructions. The slides were counterstained with hematoxylin. CD68-positive macrophages in liver and lung sections were counted

manually in 10 images (305 × 228 μ m/image) randomly selected from each mouse ($n = 3$ –5 mice).

GCCase Stability in Serum—IFG effects on GCCase stability in serum were determined using hGCCase (imiglucerase). hGCCase was added to mouse serum (pH 7.4) at 1 μ g/ml with or without IFG (25 or 50 μ M). The mixture was preincubated on ice for 10 min, then transferred to 37 °C, and incubated for the indicated time (1–7 h). At each hour, 10 μ l of each sample was removed to a new vial and diluted by 4 × 10⁴-fold with reaction buffer (0.25% sodium taurocholate, 0.25% Triton X-100, 25 mM citrate, 50 mM phosphate, pH 5.6) to achieve [IFG] <0.65 or 1.25 nM, and then GCCase activity was determined as described (22). hGCCase incubated in the reaction buffer (pH 5.6) was assayed in parallel as a control. The assay was conducted with duplicate samples in triplicate.

Glycosphingolipid Analyses—Mouse tissue samples (~60 mg wet weight) were homogenized with a PowerGen 35 (Fisher Scientific) in methanol/chloroform/water (3.6 ml; 2:1:0.6, v/v/v). Homogenates were shaken for 15 min and centrifuged (5 min at 1000 × g). Pellets were re-extracted with H₂O (0.7 ml) and chloroform/methanol (3 ml; 1:2, v/v). The combined extracts were centrifuged (10 min at 7000 × g). The supernatants were transferred to fresh tubes, and the solvents were evaporated under N₂. Dried samples were then dissolved in chloroform/methanol/water (5 ml; 2:1:0.15, v/v/v) and subjected to alkaline methanolysis (23) followed by elution from Sephadex G-25 fine columns to remove non-lipid contaminants.

The extracted samples were redissolved in methanol containing an internal standard. GC and GS analyses were carried out by electrospray ionization-LC-MS/MS using a Waters Quattro Micro API triple quadrupole mass spectrometer interfaced with an Acquity UPLC system. Optimized parameters for GC and GS were determined with individual standard compounds. For quantification of GCs, electrospray ionization-MS/MS was operated in the multiple reaction monitoring modes to monitor the transition pair of the individual protonated parent ions and their common daughter ion m/z 264. GS was monitored by mass transition m/z 462.3 → 282.4. Calibration curves were built for C16, C18, and C24:1 GCs using C12-GC as an internal standard (Avanti Polar Lipids, Inc., Alabaster, AL). Resolution of GC and galactosylceramide in brain samples was achieved using a silica column (Supelco 2.1 × 250 mm) running under hydrophobic interaction liquid chromatography mode with a mobile phase of acetonitrile/methanol/acetic acid (97:2:1, v/v/v) with 5 mM ammonium acetate. The quantification of GCs with various chain lengths was realized by using the curve of the natural GC with the most similar fatty acid chain length. The quantification of GS was based on the curve using C8-GC as internal standard (Avanti Polar Lipids, Inc.). The linear responses for GCs and GS were in the range of 50 pg to 25 ng. Two to four samples for each cohort were included in the analysis. Data were analyzed by Student's *t* test using GraphPad Prism 5 software.

Quantitation of Tissue and Serum IFG Levels—Frozen tissue samples were homogenized (7 μ l of deionized water/1 mg of tissue) using a FastPrep-24 instrument (MP Biomedicals). The homogenization was processed on the FastPrep at a speed of 4.5

Gaucher Disease Therapy

for three 30-s shakes (90 s total). Tissue homogenate (50 μ l) or serum (50 μ l) was diluted with 100 μ l of acetonitrile followed by mixing with 100 μ l of 100 ng/ml [$^{13}\text{C}_2$, ^{15}N]IFG (internal standard) dissolved in acetonitrile/methanol and 0.50% formic acid (70:30, v/v). The mixture was vortexed for 2 min and centrifuged at $15,294 \times g$ for 5 min at room temperature. Supernatant (20 μ l) was injected onto the column.

The instrument consisted of an AB SCIEX 4000 QTRAP[®] LC/MS/MS system (Foster City, CA), Shimadzu LC-10ADvp pumps, Shimadzu SIL HTc autosampler, and Shimadzu DGU-14A degasser. A Thermo Betasil Silica-100 (50 \times 3 mm; 5 μ m) was used for LC separation. The mobile phase was delivered at 0.6 ml/min with the following program: 100% A (5 mM ammonium formate and 0.05% formic acid in acetonitrile/H₂O, 95:5) for 1.2 min, linear ramp to 80% B (5 mM ammonium formate and 0.05% formic acid in methanol/water/acetonitrile, 70:20:10) in 4.3 min, holding at 80% B for 0.5 min, then increasing to 100% B in 0.01 min, and holding at 100% B for 0.49 min followed by switching to 100% A and equilibrating for 2.2 min. The MS instrument was operated in the positive multiple reaction monitoring mode with detection of the transition pairs of m/z 148.1 \rightarrow 112.1 and 151.1 \rightarrow 115.1 for IFG and [$^{13}\text{C}_2$, ^{15}N]IFG, respectively. A low limit of quantitation was set at 8 ng/g of tissue and 1 ng/ml for serum.

RESULTS

IFG Inhibition of GCases—The inhibition properties of IFG were tested with purified recombinant hGCCase (imiglucerase) and the recombinant human N370S and V394L mutant GCases in media from insect cells expressing these specific GCases (22). The respective IC_{50} and calculated K_i values were 88 ± 9 and ~ 29 nM for WT and V394L and 115 ± 5 and ~ 38 nM for N370S at pH 5.5.

Ex Vivo Effects of IFG on GCases—Concentrations of IFG between 6.25 and 50 μ M in the media enhanced GCCase activities significantly in all cells tested as shown in concentration-response curves (Fig. 1A, inset). The concentrations to achieve peak activity for each mutant cell are summarized in Fig. 1A. Human and mouse N370S GCases had the same responses and were maximally increased by ~ 3.5 -fold (or to $\sim 60\%$ of untreated WT levels). IFG did not increase human L444P activity significantly at any concentration. In comparison, the mouse GCCase activities in V394L and 4L/PS-NA fibroblasts showed ~ 3 -fold increases with 25 and 12.5 μ M IFG, respectively; these enhanced activities were $\sim 50\%$ of untreated WT levels. D409H and D409V cells showed smaller maximal enhancement, *i.e.* 1.6- and 1.3-fold, respectively.

GCCase protein levels in WT and N370S fibroblasts were maximally increased 1.3- and 1.4-fold, respectively, by IFG treatment (Fig. 1B). A 3-fold increase of GCCase protein was observed in IFG-treated L444P cells. The CRIM specific activity (activity/nmol of GCCase protein) was used to estimate the change in catalytic rate constant for the various GCases following IFG treatment. No effect on WT was found (*i.e.* the GCCase protein and activity increased concordantly), whereas with N370S, the value was increased by 2.7-fold, but that for L444P decreased to 0.36. For the mouse fibroblasts, small decreases or increases in CRIM-specific activity were observed, thereby indicating rela-

tively concordant increases in activity and protein with IFG treatment (Fig. 1B). These data show that the major effects of IFG are to stabilize the mutant GCCase protein in fibroblasts, suggesting that relatively minor conformational changes affect the catalytic rate constant as evidenced by the N370S structure (24). For the highly unstable L444P enzyme, IFG treatment did increase the amount of GCCase protein but had little to no effect on the catalytic properties of the enzyme.

To evaluate the effects of IFG on GCCase intracellular trafficking, fibroblasts were treated with IFG (50 μ M). Human and mouse WT cells with or without IFG showed colocalization of GCCase and Lamp1, a lysosomal marker (Fig. 2). In IFG-treated L444P cells, the GCCase signals were clearly increased and more robust than those in untreated cells, and IFG treatment resulted in partial lysosomal localization. For human N370S fibroblasts, the effect of IFG was similar to WT (data not shown). In mouse 4L/PS-NA cells, IFG increased V394L GCCase protein trafficking into lysosome (Fig. 2B).

In Vivo IFG Effects—The mice were administered IFG (30 mg/kg/day). For WT and homozygous V394L (4L) mice, this was started at postnatal day 10 and continued for 5 weeks. Homozygous D409H (9H) and D409V (9V) mice began treatment at 3 weeks of age, and treatment continued for 4 or 8 weeks. GCCase activities in liver, spleen, lung, and brain were compared with those of untreated mice (Fig. 3). IFG treatment had variable effects (<2 -fold) on GCCase activity in the visceral tissues (liver, lung, and spleen) of WT, 4L, 9H, and 9V mice and minor effects in the CNS of WT, 9H, and 9V mice. No IFG effect was evident in the 4L brain.

IFG Stabilized GCCase in Tissues and Serum—The hG/4L/PS-NA mouse model contains the hGCCase whose expression is under control of the Tet-Off system (14). In the absence of DOX, transgenic hGCCase is expressed and secreted from the liver in large amounts. GCCase is rapidly denatured at neutral pH (25). Following exposure to pH 7.4 in the serum, only $\sim 8\%$ of the secreted enzyme remained active (14). To test whether IFG could stabilize the secreted hGCCase, the sera from IFG-treated (30 mg/kg/day; 4 weeks) hG/4L/PS-NA mice were analyzed for GCCase activity and protein. Compared with untreated mice, serum GCCase activity and protein in the treated mice increased 2.2- and 2.4-fold, respectively (Fig. 4, A and B). The results indicate a concordant stabilization of GCCase activity and protein by IFG at neutral pH.

In vitro assays were performed to evaluate the effect of IFG on GCCase in the serum. hGCCase (imiglucerase) was incubated in mouse serum (pH 7.4) at 1 μ g/ml with or without IFG (25 μ M) at 37 $^\circ\text{C}$ for the indicated time (1–7 h). hGCCase in serum (pH 7.4) with IFG 25 μ M had a $t_{1/2}$ of ~ 2 h, and the activity was decreased to 7% of the initial activity by 7 h. In comparison, the $t_{1/2}$ was <1 h without IFG, and the activity was decreased to $<5\%$ by 3 h. As a control, the enzyme incubated in the reaction buffer alone at pH 5.6 (lysosomal pH) had a $t_{1/2}$ of ~ 6 h, remained at 80% of initial activity after 3 h of incubation, and was only reduced to 50% by 7 h. The result indicates that the enzyme was not stable at neutral pH 7.4, and IFG increased the stability of the liver hGCCase secreted into the serum.

Feeding DOX to these mice turns off hGCCase expression in liver, and the remaining GCCase activity in tissues is that of the

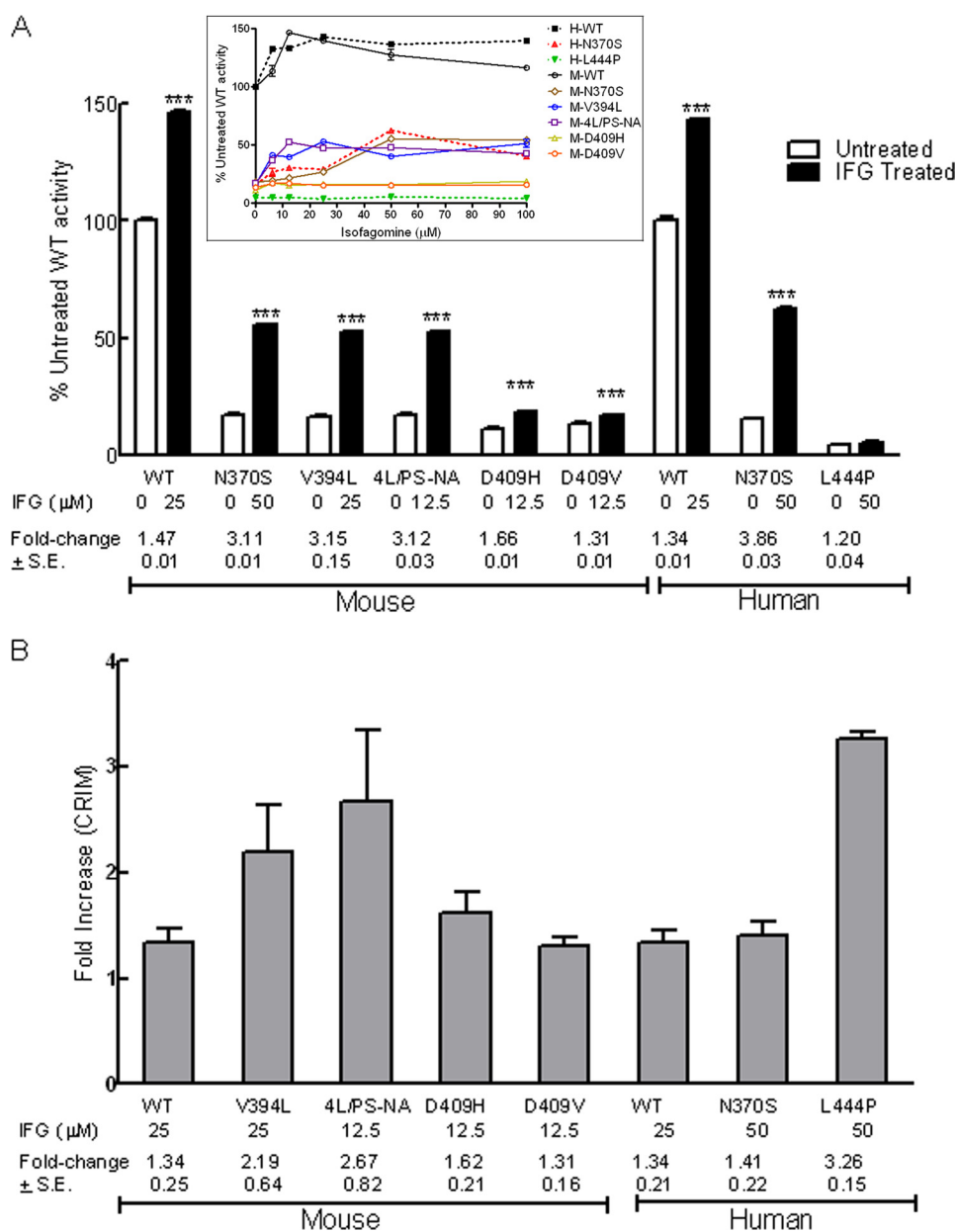


FIGURE 1. IFG effects on fibroblast GCase activity (A) and protein (B) levels. A, mouse (M) (WT, N370S, V394L, 4L/PS-NA, D409H, and D409V) and human (H) (WT, N370S, and L444P) fibroblast cells were incubated with IFG. GCase activity at the indicated concentration to achieve peak effects (see *inset*) is presented as the percentage of untreated WT activity. All treated mouse and human WT and mutant cells except L444P showed significant increases of activity. The activities in treated mouse V394L and 4L/PS-NA increased to ~50% of WT levels. GCase activity in IFG-treated human N370S cells was enhanced to 60% of WT levels. -Fold changes relative to the untreated cells are indicated. The experiments were done in triplicate. Data were analyzed by Student's *t* test. ***, $p < 0.001$. *Inset*, IFG concentration-response curves for human and mouse WT and mutant GCases in fibroblasts. The cells were treated with IFG at the indicated concentrations for 5 days. GCase activity changes after IFG treatment are presented as a percentage of untreated WT activity for mouse or human, respectively. B, quantitation of GCase protein in each variant was determined immunologically with mouse- or human-specific antibodies. All IFG-treated cells showed increases in GCase protein levels. These are presented as -fold change (indicated below the columns) relative to the untreated cells. The results and error bars represent the mean \pm S.E. ($n = 3$).

mouse V394L enzyme. Neither the WT nor mutant mouse GCases are secreted from cells under non-overexpressed conditions (14, 16). Consequently, the effects of IFG treatment on either the human WT or mouse V394L GCase activities and proteins can be determined by feeding mice DOX-free or DOX-containing food. At 4 weeks of age, hG/4L/PS-NA mice were fed IFG in drinking water for 4 weeks on either DOX or DOX-free food. DOX-free mice showed an increase of GCase (hGCase + V394L GCase) activity in the lung (7.6-fold) and spleen (2.1-fold) after IFG treatment (Fig. 5A). The GCase

activity in IFG-treated livers showed a trend toward increases relative to the untreated mice; this may be due to the very large amounts of hGCase produced in the transgenic livers. In DOX-treated hG/4L/PS-NA mice, IFG did increase V394L GCase activity in the liver (3.8-fold) but not in the lung and spleen (Fig. 5A).

The specificity of our antibodies to human or mouse GCase allowed independent quantification of the human or mouse proteins under all experimental conditions. Compared with untreated mice, the hGCase protein level in IFG-treated liver

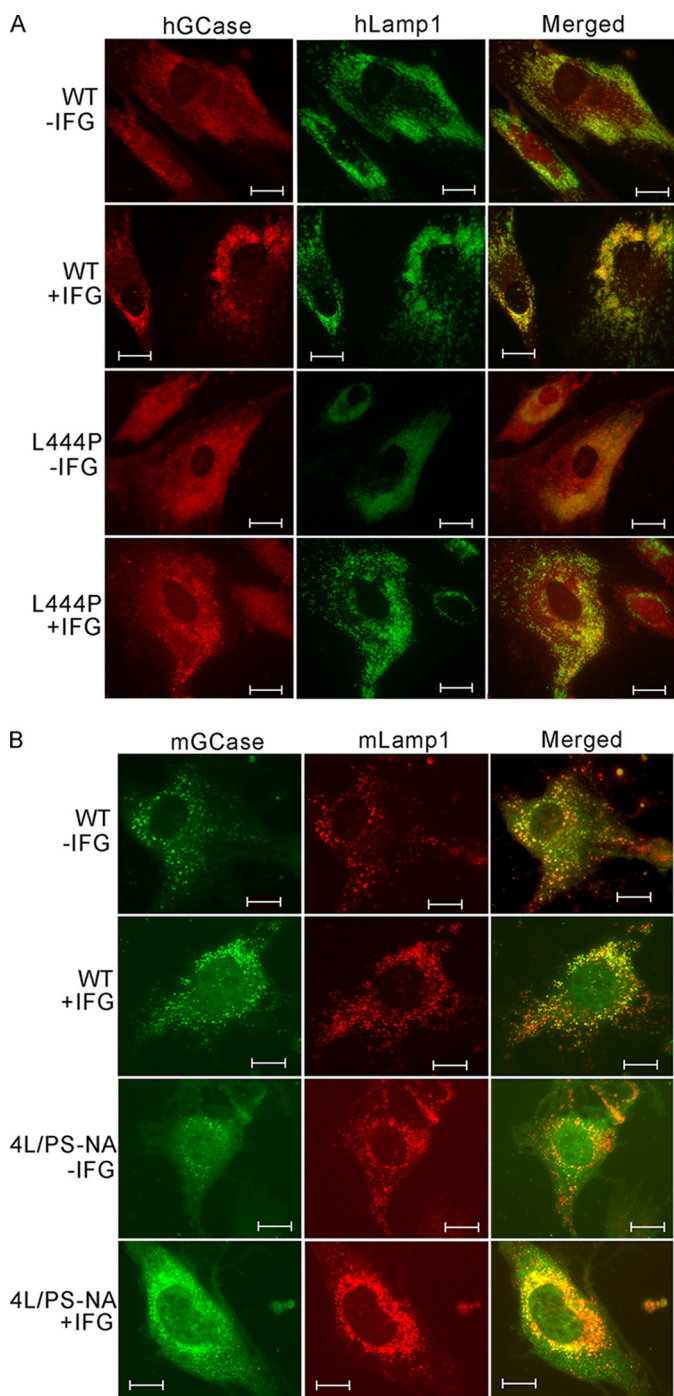


FIGURE 2. Cellular localization of GCases in IFG-treated fibroblasts. Colocalization of hGCCase (A) (red) with lysosomal marker human Lamp 1 (green) and mouse GCCase (mGCCase) (B) (green) with mouse Lamp1 (red) was conducted by immunofluorescence staining. The fibroblast cells were treated with IFG (50 μ M). Both untreated (-IFG) and treated (+IFG) human and mouse WT GCases colocalized with Lamp1 in the lysosome. The untreated human L444P GCCase was nearly undetectable. In contrast, the treated L444P cells had increased GCCase and trafficking to the lysosome. In IFG-treated mouse 4L/PS-NA cells, the GCCase signal was enhanced and localized in the lysosome. Scale bars, 10 μ m.

increased by 2.6-fold, and in the spleen, it increased by 1.3-fold. In the lung, hGCCase protein was present in the IFG-treated mice, whereas it was undetectable in the untreated mice (Fig. 5B). In IFG-treated mice, the V394L GCCase protein increased by 2.1-fold in the liver, 1.6-fold in the lung, and 1.4-fold in the

spleen (Fig. 5C). These results indicated that IFG stabilizes hGCCase derived from serum and the endogenous mouse V394L mutant proteins and enhances their enzymatic activities to varying degrees in different organs. The delivery of hGCCase present in the serum to the lung and spleen was enhanced by IFG. Importantly, the activity in the lung was increased more than the protein (Fig. 5, A and B), thereby suggesting a reformation of the enzyme by IFG during synthesis and secretion from the liver.

IFG Levels in Mouse Tissues and Serum—The samples from hG/4L/PS-NA mice treated with IFG in drinking water were collected at the end of 4 or 8 weeks of treatment (see GCCase activity and lipid data shown in Figs. 5, 6, 7, and 8). IFG levels in tissues and serum were determined by LC/MS. The liver had the highest IFG level. The tissue IFG level was in the following order: liver > serum > lung > brain (Table 1). IFG levels were not significantly different between 4 and 8 weeks of treatments. The mice without IFG treatment had no detectable IFG in tissues or serum. The relative IFG tissue levels were consistent with those reported in L444P mutant tissues (21).

In Vivo Effects of IFG Treatment on Lipid Storage—In the absence of DOX (DOX-free), hGCCase reduced substrate levels in 4L/PS-NA mouse tissues. Turning off hGCCase expression with dietary DOX led to substrate accumulation (Fig. 6) (14). For these experiments, hG/4L/PS-NA mice started IFG treatment at 4 weeks for either DOX or DOX-free groups. This treatment was continued for 4 (Fig. 6) or 8 weeks (Fig. 7). No significant changes in substrate levels were observed in 4-week IFG-treated mice except that lung GS levels were reduced by 46% compared with those mice that received only DOX (Fig. 6). In 8-week IFG-treated DOX mice, both GC and GS were reduced by 35–40% in liver and lung (Fig. 7, A and B). However, decreases in GC (75%) and GS (62%) levels were observed in the lungs of DOX-free mice receiving IFG. The GC and GS levels in the liver of these DOX-free mice were very low, and changes could not be appreciated by the addition of IFG. The substrate reductions correlated with activity increases in IFG-treated mice (Fig. 7C). CD68-positive storage cells were quantified in liver and lung from each group of mice. Decreased numbers of storage cells were detected in the lungs only of DOX-free mice receiving IFG treatment (Fig. 7D). Consequently, the reduction of storage cells correlated with >50% decreases of substrate levels. In the brain, the transgenic hGCCase activity (*i.e.* DOX-free) was slightly enhanced, and V394L GCCase activity (*i.e.* DOX-treated) was unchanged by IFG treatment (Fig. 7), but GC and GS levels in the brain were not significantly altered by IFG treatment (Fig. 7).

The ability to turn on and off hGCCase synthesis in the liver permitted an evaluation of the extent to which IFG influenced V394L mouse GCCase or newly synthesized hGCCase. hG/4L/PS-NA mice were kept on DOX for 4 weeks (*i.e.* between 3 and 7 weeks of age) and then taken off DOX and treated with IFG for 4 weeks. In these animals, IFG led to further reductions (50–54%) in GC levels in the liver and lung, whereas GS reductions were detected only in the lung (Fig. 8, A and B). The lack of an effect on liver GS levels is likely attributable to concentrations of GS near the noise level in liver before IFG treatment, thereby obscuring any additional effects (Fig. 8B). There was an inverse

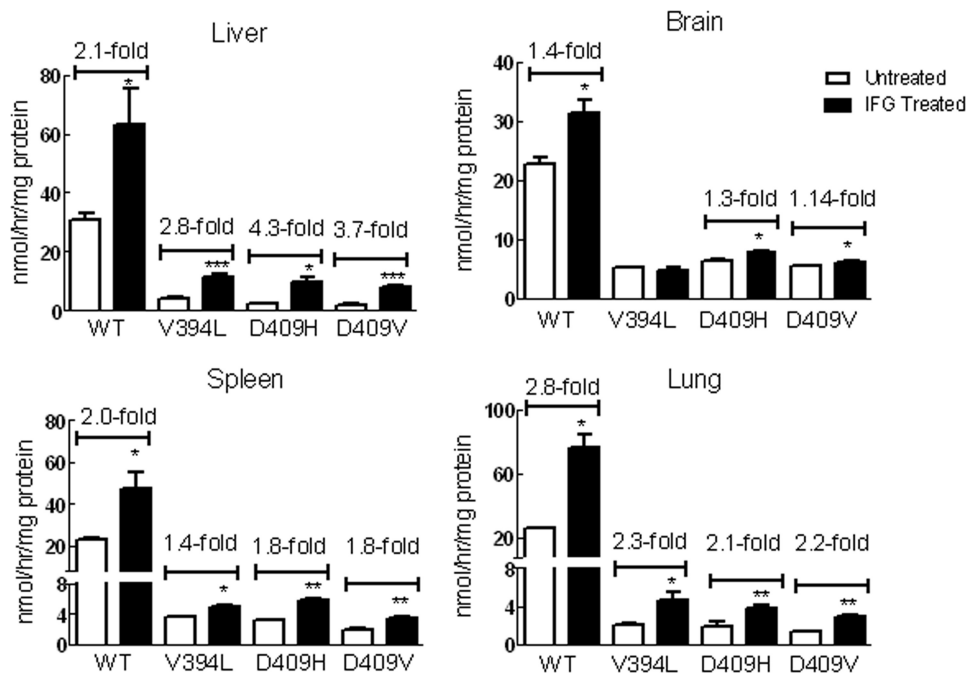


FIGURE 3. IFG treatment enhanced GCase activity in mouse tissues. The mice were administered IFG (30 mg/kg/day) in drinking water. The treatments for WT and V394L mice were started at postnatal day 10 and continued for 5 weeks; for D409H mice, the treatment started at 21 days and continued for 4 weeks; and for D409V mice, the treatment started at 23 days and continued for 8 weeks. GCase activities in each tissue were significantly increased in IFG-treated WT and mutant mice tissues except V394L brain. Data were analyzed by Student's *t* test. *, $p < 0.05$; **, $p < 0.01$; ***, $p < 0.001$. The results and error bars represent the mean \pm S.E. ($n = 3$ mice).

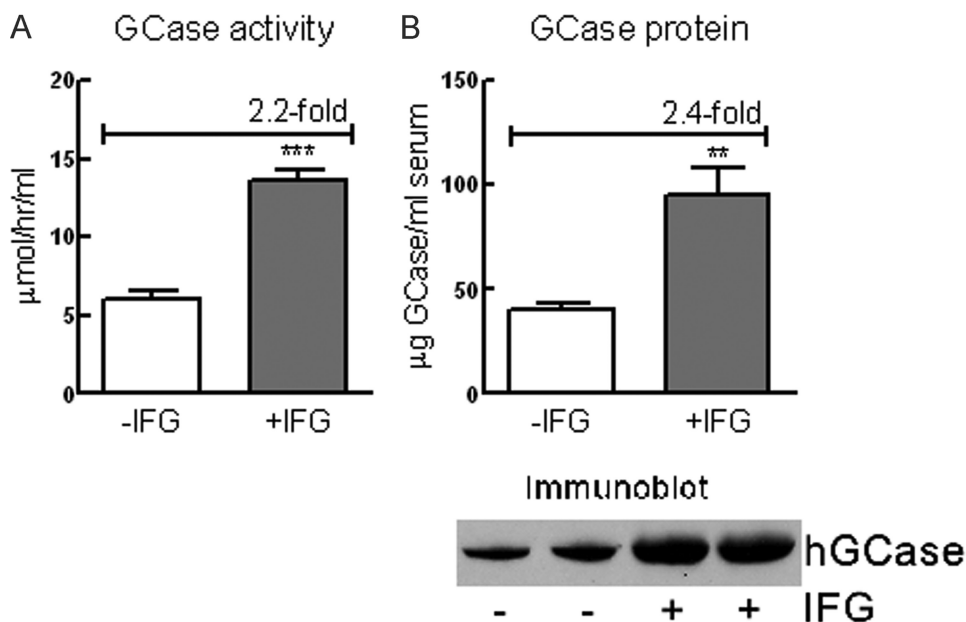


FIGURE 4. IFG stabilized GCase protein in serum. The hGCCase is expressed in and secreted from hG/4L/PS-NA mouse livers. *A*, in IFG-treated mice (30 mg/kg/day for 4 weeks) hGCCase activities secreted into the serum were significantly increased compared with untreated mice. *B*, immunoblot of GCase in serum determined by anti-hGCCase antibody and quantitated relative to known amounts of imiglucerase as standard. Human GCase protein in the serum from IFG-treated mice was significantly increased compared with the untreated mice. Data were analyzed by Student's *t* test (duplicate assays). **, $p < 0.01$; ***, $p < 0.001$. The results and error bars represent the mean \pm S.E. ($n = 3$ mice).

correlation of substrate reduction and enhancement of GCase activity in IFG-treated liver and lung (Fig. 8C). The decrease in CD68-positive cells correlated with the changes in substrate levels (Fig. 8D). This result suggests that IFG has an effect on stabilizing the GCase conformation in the liver and lung during its synthesis. The minor increase of brain hGCCase activity (Fig. 7) in IFG-treated mice likely resulted from hGCCase in the blood

due to incomplete perfusion. Such a low level of activity had no effect on the reduction of substrate levels in the brain (Fig. 8).

DISCUSSION

Small molecule competitive inhibitors of lysosomal enzymes have been envisioned as potential "chaperones" for the improvement of residual mutant activity (enzyme enhance-

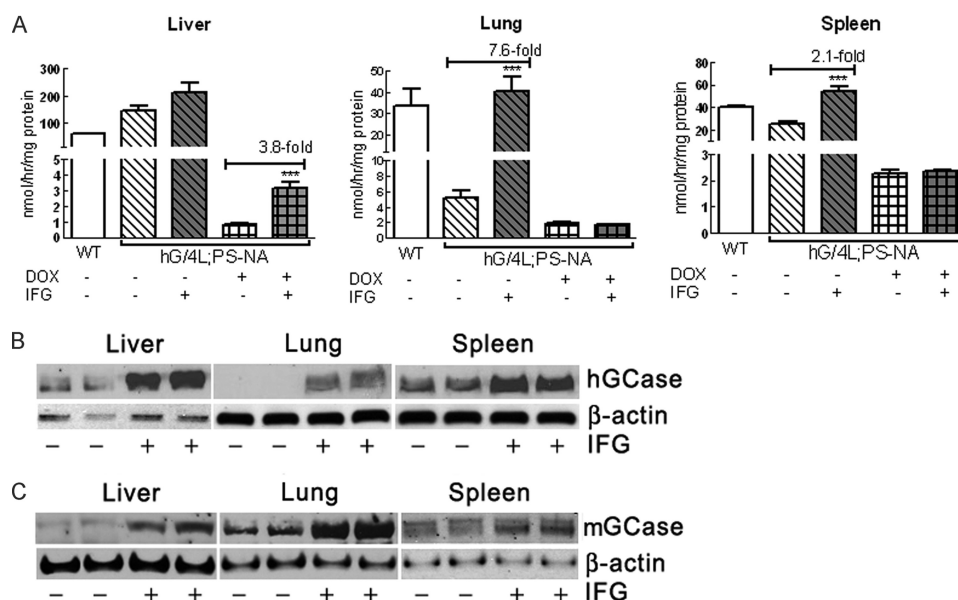


FIGURE 5. **GCase activity and protein in IFG-treated hG/4L/PS-NA mice.** Human GCase was expressed in the liver of hG/4L/PS-NA mice when fed DOX-free food. In the mice on DOX food, hGCase expression was turned off; residual activity was from mouse V394L mutant GCase. *A*, IFG treatment for 4 weeks in drinking water enhanced both hGCase and mouse V394L mutant GCase activities in the liver and hGCase activity in the lung and spleen (gray bars). *B*, immunoblot using anti-hGCase antibody demonstrated that IFG treatment for 4 weeks increased hGCase protein levels in the liver, lung, and spleen of hG/4L/PS-NA mice. No protein was detected in untreated lung. *C*, immunoblot of mouse GCase detected by anti-mouse GCase antibody showed increases of mouse GCase (mGCase) protein in treated liver, lung, and spleen. β -Actin was the loading control. Data were analyzed by Student's *t* test. ***, $p < 0.001$. The results and error bars represent the mean \pm S.E. ($n = 3$ mice).

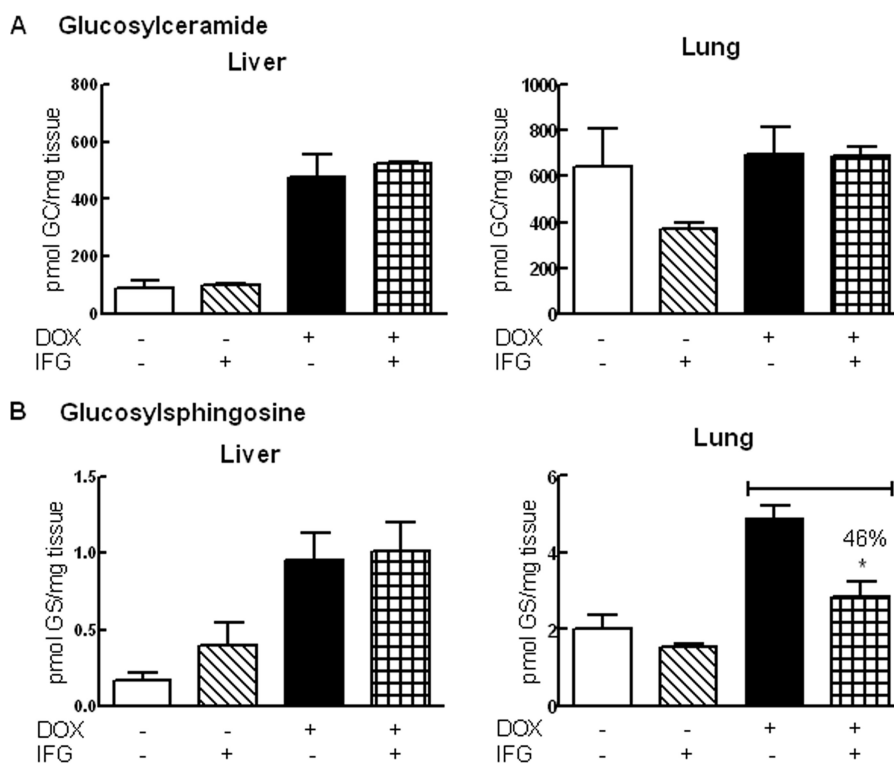


FIGURE 6. **Effects of IFG treatment for 4 weeks in hG/4L/PS-NA mice.** The mice were treated with IFG for 4 weeks with DOX-free or DOX food. *A*, no significant changes of GC levels were observed in IFG-treated liver and lung. *B*, in liver of DOX-free IFG-treated mice, GS was increased. In lungs of DOX and IFG-treated mice, GS was decreased. The liver GS level was not altered in these same mice. GC and GS levels were quantitated by LC/MS and normalized by mg of wet tissues. Data were analyzed by Student's *t* test. *, $p < 0.05$. GCase activities for these samples are presented in Fig. 5. The results and error bars represent the mean \pm S.E. ($n = 3$ mice).

ment therapy) in cells of individuals afflicted with such diseases (18, 26). To date, several *ex vivo* and a few *in vivo* studies have assessed the effects of such compounds on normal and mutant enzyme activities when administered via culture media or orally

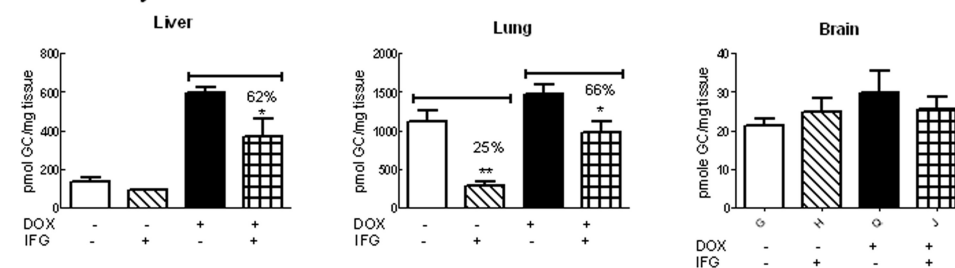
(19–21, 27, 28). In particular, for lysosomal hydrolyzes (e.g. α -galactosidase A or GCase), iminosugars (e.g. IFG) are potent competitive inhibitors that could act as chaperones to improve the stability and/or activity of the residual mutant enzymes in

TABLE 1
IFG levels in tissues and serum

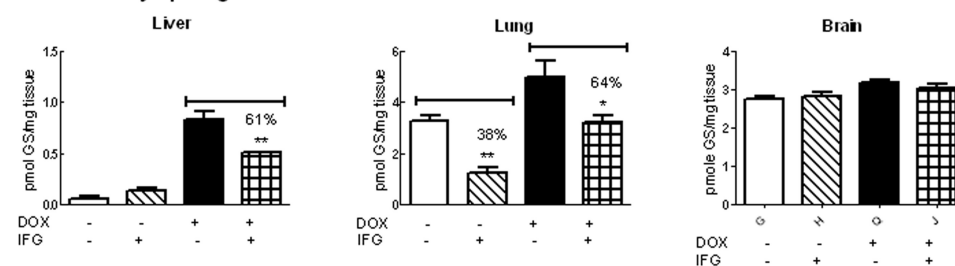
Tissues and sera were collected at the end of 4 or 8 weeks of treatment with IFG at 30 mg/kg/day in drinking water. There was no significant difference (Student's *t* test) in IFG levels in individual tissues at 4 or 8 weeks of treatment. Tissue GCase activities and lipid results at 4 weeks of treatment are presented in Figs. 5 and 6, and at those at 8 weeks of treatment are in Figs. 7 and 8. The results represent the mean \pm S.E. Numbers in parentheses indicate the number of mice.

IFG treatment weeks	IFG			Serum IFG ng/ml
	Liver	Lung	Brain	
4	206.00 \pm 20.61 (7)	29.23 \pm 9.02 (3)	13.15 \pm 0.45 (4)	42.75 \pm 22.55 (2)
8	268.50 \pm 38.40 (12)	32.47 \pm 11.43 (12)	14.76 \pm 3.83 (12)	56.24 \pm 14.00 (9)

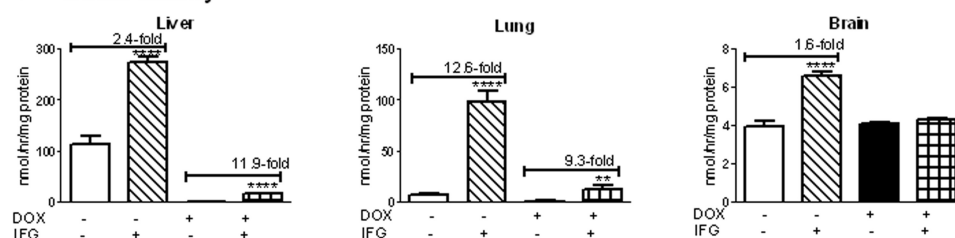
A Glucosylceramide



B Glucosylsphingosine



C GCase activity



D CD68 positive cells

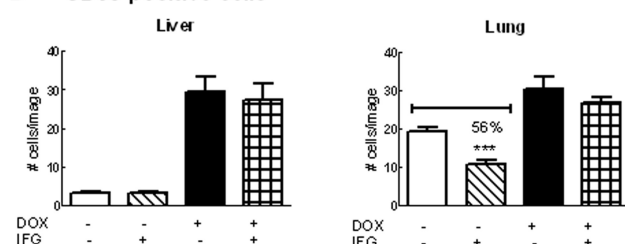


FIGURE 7. Effects of IFG treatment for 8 weeks in hG/4L/PS-NA mice. IFG was administered to the mice by drinking water for 8 weeks with the mice either on DOX or DOX-free food. *A*, the liver GC level was low in mice on DOX-free food and not significantly changed by IFG treatment. The liver GC in the mice fed with DOX food was reduced by 38% with IFG treatment. In comparison, lung GC levels were significantly reduced in IFG-treated mice on either DOX or DOX-free food. Brain GC levels were not significantly changed by IFG treatment. *B*, the liver GS level was very low in the mice on DOX-free food and not significantly altered by IFG, whereas in mice fed DOX food, GS was reduced by 39% with IFG treatment. Lung GS levels were significantly reduced in IFG-treated mice on DOX or DOX-free food. Brain GS levels were not significantly changed by IFG treatment. *C*, GCase activity. IFG treatment for 8 weeks in drinking water enhanced both hGCase (*hatched bars*) and mouse V394L mutant GCase (*checked bars*) activities in the liver and lung. IFG treatment enhanced hGCase activity (*hatched bars*) by 1.6-fold in brain but did not alter mouse V394L GCase activity (*checked bars*). *D*, the CD68-positive macrophages were counted in liver and lung sections of 8-week IFG-treated mice. Decreased cell numbers were observed in IFG-treated livers from the mice on DOX-free food. The CD68-positive cells were counted from 10 images (305 \times 228 μ m for each image) per mouse. GC and GS levels were quantitated by LC/MS and normalized by mg of wet tissues. Data were analyzed by Student's *t* test. *, $p < 0.05$; **, $p < 0.01$; ***, $p < 0.001$, ****, $p < 0.0001$. The results and error bars represent the mean \pm S.E. ($n = 3$ mice).

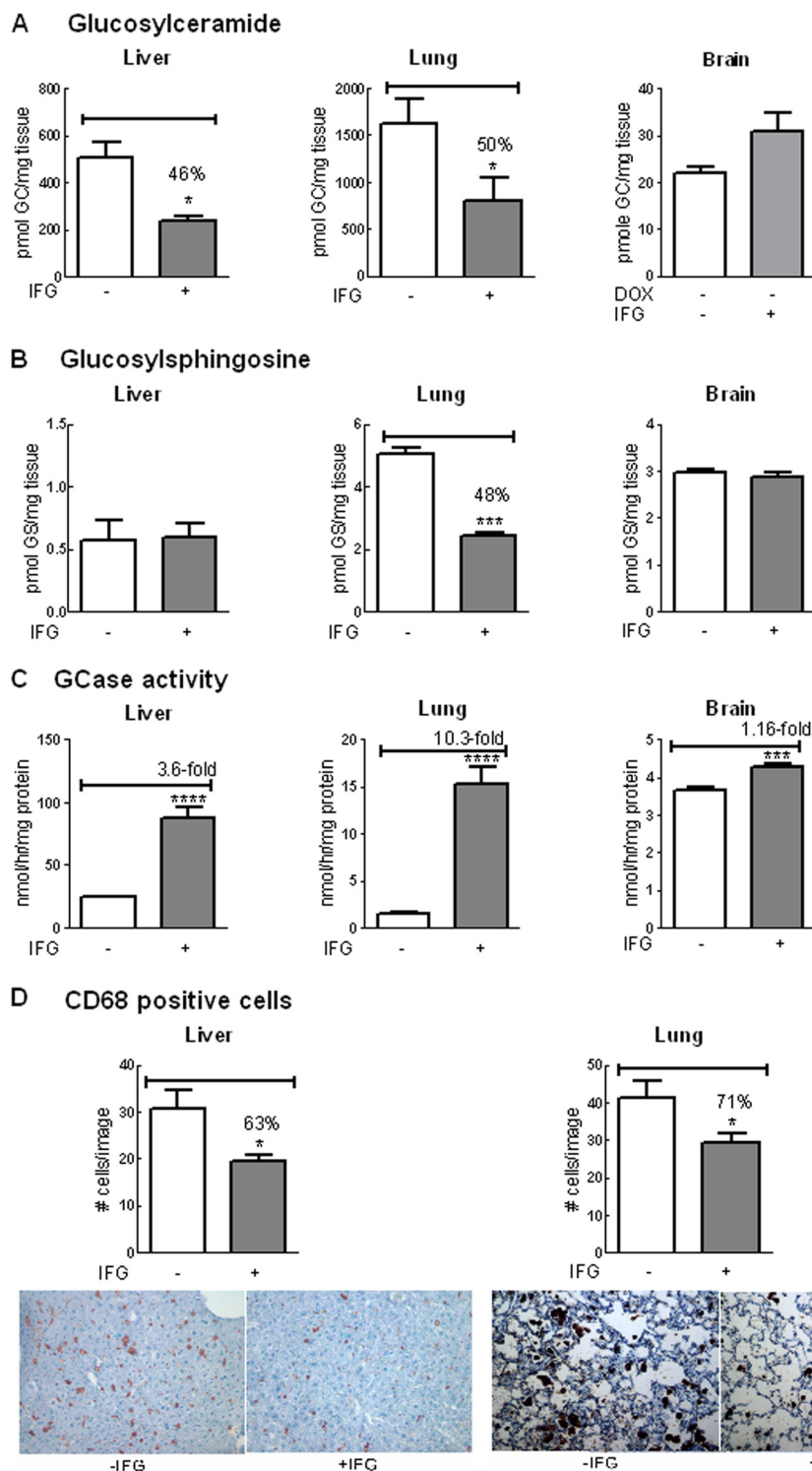


FIGURE 8. Reduced substrates and storage cells in hG/4L/PS-NA mice treated for 4 weeks with IFG during hGCse synthesis in the liver. hG/4L/PS-NA mice were placed on DOX food from 3 to 7 weeks of age to turn off hGCse expression. The mice were then withdrawn from DOX to permit hGCse synthesis and fed with IFG-containing drinking water from 7 to 11 weeks of age. *A*, GC levels in IFG-treated liver and lung were reduced. Brain GC levels were not significantly changed by IFG treatment. *B*, GS levels were decreased in IFG-treated mouse livers, lung, and brain. *C*, GCse activities were increased in IFG-treated liver, lung, and brain. *D*, CD68-positive cell numbers in IFG-treated mice were decreased in both liver (*upper panel*) and lung (*lower panel*). Images of liver and lung were stained with anti-CD68 antibody on macrophage cells (*brown*) counterstained with hematoxylin (*blue*). The cell counts and lipid level determination are as described in Fig. 7. Data were analyzed by Student's *t* test. *, $p < 0.05$; **, $p < 0.01$; ***, $p < 0.001$; ****, $p < 0.0001$. The results and error bars represent the mean \pm S.E. ($n = 3$ mice).

specific cell types (19, 20, 27). In general, these studies are based on relatively artificial assay systems in which cultured cells or removed tissues are homogenized with various buffers that lead

to significant dilutions of the reversible inhibitor. In addition, synthetic substrates and/or detergents are used to assess the effects on specific enzymes (19–21, 27). The dilution effects

either on cells or lysates clearly remove the inhibitor from the environs of the enzyme and lead to essentially an uninhibited enzyme. Remarkably, many of these studies have shown substantial increases in residual enzyme activity as measured by these assays (19–21, 27), suggesting that the mutant enzymes can retain different conformational states for some period after the dilution of the “chaperone” or reconforming molecule. In addition, iminosugars can be delivered to several locations throughout the body, including multiple intracellular and extracellular spaces with differential pH environments (20, 21, 29). The latter clearly affects the binding constants for these compounds to specific enzymes. For example, IFG has been used as a very potent inhibitor of GCCase, the Gaucher disease enzyme, and this compound has a pK_a of ~ 8.6 (30). The K_i varies substantially with pH with IFG becoming a much more potent inhibitor at more neutral pH values (31), *i.e.* K_i values of $\sim 145, 30, 20,$ and 1 nM at pH 4.5, 5.6, 6.0, and 7.2, respectively, with purified hGCCase.³ Such *ex vivo* and *in vitro* studies indicate that this compound could have differential interactions and effects in several cellular and in particular extracellular environments. Such results have implications for the conformation of intracellular enzymes, specifically GCCase, and extracellular enzymes for enzyme or gene therapy experiments in which the therapeutic enzyme is present in a hostile, potentially denaturing environment, *e.g.* plasma/serum. Because more neutral pH values denature GCCase, such a “chaperone-like” agent might be highly useful in the treatment of Gaucher disease variants using approaches that require the exposure of the enzyme to non-lysosomal pH. Critical studies of the effects on actual *in vivo* substrate accumulation by the apparent increases assessed from *in vitro* enzyme assays must be carried out for this approach to have viability in the lysosomal disease treatment paradigms.

Our data demonstrate that IFG is a highly potent inhibitor of human and murine WT and selected mutant GCases. These effects are comparable with mouse GCCase and hGCCase, which differ by about 15% in amino acid sequence. Both the enhancement effects of IFG on WT and mutant GCCase activity and their stabilities were similar within the murine or human fibroblast environments. In addition, each of the several different mutant GCases used in these experiments shows differential effects of IFG on enzymatic activity, cell distribution, and the stability of the GCases within cells. Importantly, the V394L and N370S GCCase activities and proteins were enhanced by IFG *ex vivo* to nearly heterozygous levels, which should be therapeutic *in vivo*.

In vivo IFG was shown to have variable effects on the WT and mutant GCases in different tissues with the effects in liver \geq lung \geq spleen \geq brain *vis-à-vis* GCCase activity and protein levels. In these tissues, particularly liver and lung, a correspondence was observed between the degree of response of mutant GCases with that in cultured skin fibroblasts, suggesting a potential utility to predict *in vivo* effects. The differential tissue effects of IFG could have several etiologies, but the most likely would be the greater uptake into the various tissues with the amount delivered to liver $>$ lung $>$ spleen $>$ brain. However, some effects were observed in all tissues.

The above studies provide a backdrop for the evaluation of the *in vivo* effects of IFG on WT and mutant GCases and for determining effects on substrate accumulation. Our transgenic system that contains the doxycycline-responsive element for expression of hGCCase in liver (14) allowed us to examine IFG in conjunction with either enzyme or gene therapy approaches. The degree of IFG effects on the hepatically expressed hGCCase was similar to that of the endogenous mouse WT GCCase in the respective livers, spleens, and lungs. Importantly, the removed tissues had been perfused with saline so that hGCCase-rich plasma was eliminated, thereby permitting assessments only of the enzyme that was taken up into the tissue. Consistent with the tissue IFG distribution levels, liver $>$ lung $>$ brain, the effects of IFG were specific to the tissue with large effects on increasing hGCCase activity in the liver (3–5 times) and also 3–4-fold increases in mutant V394L GCCase. In lung, very large effects were seen on the hGCCase with little effect on the endogenous mutant enzyme V394L. In spleen and brain, a lesser but significant effect occurred with the hGCCase, but no effect was detected on the endogenous V394L GCCase, indicating that these tissues were exposed to lower concentrations of IFG. As an example, there was a lack of major effect from IFG treatment in the CNS of a V394L-based model (28).

Importantly, together with the GCCase activities, the enzyme proteins were also increased by IFG treatment in all tissues. However, disproportionate increases were found in the GCCase proteins compared with the respective activities in all tissues except the liver. These results indicate that IFG stabilized the WT human and mutant murine GCases against proteolysis and that IFG had less effect on conformations that restore or increase enzymatic activities. Plasma that contained high levels of hGCCase in the mice that were off DOX showed increases in hGCCase activities when IFG was also administered. This was further shown by *in vitro* assays in which IFG diminished the rapid inactivation of GCCase activity in serum. This indicates substantial protection afforded by IFG to the hGCCase from denaturation by plasma pH.

The ultimate aims of treatments are to decrease storage of GC and GS in all tissues and improve the health of patients with these diseases. In particular, the tissue-specific changes of GC and GS were partially correlated with the GCCase activity effects. In the DOX-free transgenic mice receiving IFG, there was little effect on the substrate accumulation in the liver. Significant decreases in GC levels were observed in the lung. In the same mice, GS increased significantly in the liver (Fig. 6B), whereas this substrate was decreased in the lung, suggesting greater exposure of the liver to IFG, which was apparently at inhibitory concentrations for this poor substrate, *i.e.* GS is cleaved at ~ 100 – 200 times lesser rates than GC (32). The paradoxical result in the lung could have resulted from a lower level of IFG present in the tissue, leading to enhanced GCCase activity without significant inhibitory effects on either substrate. When these transgenic mice were put on DOX as well as IFG, only the mutant V394L enzyme is present, and some decreases in GS concentrations were seen in various tissues.

In comparison, 8 weeks of IFG treatment resulted in substantially different effects. These effects were not dependent on IFG concentration because there was no significant difference of

³ B. Liou and G. A. Grabowski, unpublished data.

IFG levels in each tissue between 4 and 8 weeks of treatment. In the liver of DOX-free mice, IFG effects were obscured because very low levels of GC and GS were present (probably non-lysosomal) because of the high level expression of human WT GCCase. In the lungs, the large amounts of GC and GS, particularly the latter, showed decreases relative to the IFG-untreated mouse. However, the GS levels obtained in the IFG-treated mice were nearly the same as in the 4-week treated mice. Reductions of GC and GS levels were correlated with an increase of GCCase activity in those treated tissues. This suggests that the effect was either due to IFG enhancing enzyme activity (e.g. k_{cat}) and/or to amounts of enzyme that prevent substrate accumulation. Importantly, these changes in lung glycolipid content were not observed in similar mice treated with intravenous enzyme therapy products in which no effect on lung lipid accumulation was observed (33).

The ability to administer IFG after doxycycline had been present for some period allowed, upon DOX withdrawal, the new synthesis of hGCCase in the presence of IFG, leading to some additional enhancement of activity. This result suggests that IFG may be useful during the synthesis of GCCase as well as postsynthetically for conformational retention/promotion effects. The effects of this newly synthesized enzyme on substrate hydrolysis was somewhat better than that observed at 8 weeks for hGCCase that had been performed prior to the addition of IFG (Fig. 8).

These results support the contention that an active site-directed inhibitor can enhance endogenous visceral wild-type or mutant enzyme activity, i.e. GCCase, *in vivo*, but the effects are tissue-specific. These results could be due to the differential exposure of tissue GCCase to IFG, e.g. liver > serum > lung > brain, and/or a differential response of the GCCase in various tissues or to intrinsically different properties of the enzyme in the tissue environments. Finally, the results suggest that the effects of IFG are greater on enzyme synthesized in the presence of IFG rather than in a postsynthetic state. This implies that a coformulation of such enzymes while the enzyme is being made in various bioreactors might provide specific enhancement that cannot be obtained after the enzyme is fully formed. This would have implications for the dosing and treatment for enzymes that are responsive to such agents.

Acknowledgments—We thank Lori Stanton, Huimin Ran, Venette Inskip, Matt Zamzow, Rebecca Coyle, and Rachel Reboulet for technical assistance; Lisa McMillin and Sabina Sylvest for skilled tissue preparation; and Michelle Cooley for clerical expertise.

REFERENCES

- Grabowski, G. A., Petsko, G., and Kolodny, E. H. (2010) in *The Online Metabolic and Molecular Bases of Inherited Diseases* (Valle, D., Beaudet, A. L., Vogelstein, B., Kinzler, K. W., Antonarakis, S. E., Ballabio, A., Scriver, C. R., Sly, W. S., and Childs, B., eds) 9th Ed., Chapter 146, McGraw-Hill, New York
- Koprivica, V., Stone, D. L., Park, J. K., Callahan, M., Frisch, A., Cohen, I. J., Tayebi, N., and Sidransky, E. (2000) Analysis and classification of 304 mutant alleles in patients with type 1 and type 3 Gaucher disease. *Am. J. Hum. Genet.* **66**, 1777–1786
- Horowitz, M., Wilder, S., Horowitz, Z., Reiner, O., Gelbart, T., and Beutler, E. (1989) The human glucocerebrosidase gene and pseudogene: structure and evolution. *Genomics* **4**, 87–96

- Kolodny, E. H., Ullman, M. D., Mankin, H. J., Raghavan, S. S., Topol, J., and Sullivan, J. L. (1982) Phenotypic manifestations of Gaucher disease: clinical features in 48 biochemically verified type 1 patients and comment on type 2 patients. *Prog. Clin. Biol. Res.* **95**, 33–65
- Volk, B. W., Wallace, B. J., and Adachi, M. (1967) Infantile Gaucher's disease: electron microscopic and histochemical studies of a cerebral biopsy. *J. Neuropathol. Exp. Neurol.* **26**, 176–177
- Charrow, J., Andersson, H. C., Kaplan, P., Kolodny, E. H., Mistry, P., Pastores, G., Rosenbloom, B. E., Scott, C. R., Wappner, R. S., Weinreb, N. J., and Zimran, A. (2000) The Gaucher registry: demographics and disease characteristics of 1698 patients with Gaucher disease. *Arch. Intern. Med.* **160**, 2835–2843
- Tsuji, A., Omura, K., and Suzuki, Y. (1988) Intracellular transport of acid α -glucosidase in human fibroblasts: evidence for involvement of phosphomannosyl receptor-independent system. *J. Biochem.* **104**, 276–278
- Eyal, N., Wilder, S., and Horowitz, M. (1990) Prevalent and rare mutations among Gaucher patients. *Gene* **96**, 277–283
- Pasmanik-Chor, M., Laadan, S., Elroy-Stein, O., Zimran, A., Abrahamov, A., Gatt, S., and Horowitz, M. (1996) The glucocerebrosidase D409H mutation in Gaucher disease. *Biochem. Mol. Med.* **59**, 125–133
- Theophilus, B., Latham, T., Grabowski, G. A., and Smith, F. I. (1989) Gaucher disease: molecular heterogeneity and phenotype-genotype correlations. *Am. J. Hum. Genet.* **45**, 212–225
- Xu, Y. H., Quinn, B., Witte, D., and Grabowski, G. A. (2003) Viable mouse models of acid β -glucosidase deficiency: the defect in Gaucher disease. *Am. J. Pathol.* **163**, 2093–2101
- Liu, Y., Suzuki, K., Reed, J. D., Grinberg, A., Westphal, H., Hoffmann, A., Döring, T., Sandhoff, K., and Proia, R. L. (1998) Mice with type 2 and 3 Gaucher disease point mutations generated by a single insertion mutagenesis procedure. *Proc. Natl. Acad. Sci. U.S.A.* **95**, 2503–2508
- Sun, Y., Quinn, B., Witte, D. P., and Grabowski, G. A. (2005) Gaucher disease mouse models: point mutations at the acid β -glucosidase locus combined with low-level prosaposin expression lead to disease variants. *J. Lipid Res.* **46**, 2102–2113
- Sun, Y., Quinn, B., Xu, Y. H., Leonova, T., Witte, D. P., and Grabowski, G. A. (2006) Conditional expression of human acid β -glucosidase improves the visceral phenotype in a Gaucher disease mouse model. *J. Lipid Res.* **47**, 2161–2170
- Cullen, V., Sardi, S. P., Ng, J., Xu, Y. H., Sun, Y., Tomlinson, J. J., Kolodziej, P., Kahn, L., Saftig, P., Woulfe, J., Rochet, J. C., Glicksman, M. A., Cheng, S. H., Grabowski, G. A., Shihabuddin, L. S., and Schlossmacher, M. G. (2011) Acid β -glucosidase mutants linked to Gaucher disease, Parkinson disease, and Lewy body dementia alter α -synuclein processing. *Ann. Neurol.* **69**, 940–953
- Leonova, T., and Grabowski, G. A. (2000) Fate and sorting of acid β -glucosidase in transgenic mammalian cells. *Mol. Genet. Metab.* **70**, 281–294
- Yu, Z., Sawkar, A. R., and Kelly, J. W. (2007) Pharmacologic chaperoning as a strategy to treat Gaucher disease. *FEBS J.* **274**, 4944–4950
- Fan, J. Q., Ishii, S., Asano, N., and Suzuki, Y. (1999) Accelerated transport and maturation of lysosomal α -galactosidase A in Fabry lymphoblasts by an enzyme inhibitor. *Nat. Med.* **5**, 112–115
- Lieberman, R. L., Wustman, B. A., Huertas, P., Powe, A. C., Jr., Pine, C. W., Khanna, R., Schlossmacher, M. G., Ringe, D., and Petsko, G. A. (2007) Structure of acid β -glucosidase with pharmacological chaperone provides insight into Gaucher disease. *Nat. Chem. Biol.* **3**, 101–107
- Stee, R. A., Chung, S., Wustman, B., Powe, A., Do, H., and Kornfeld, S. A. (2006) The iminosugar isofagomine increases the activity of N370S mutant acid β -glucosidase in Gaucher fibroblasts by several mechanisms. *Proc. Natl. Acad. Sci. U.S.A.* **103**, 13813–13818
- Khanna, R., Benjamin, E. R., Pellegrino, L., Schilling, A., Rigat, B. A., Soska, R., Nafar, H., Ranes, B. E., Feng, J., Lun, Y., Powe, A. C., Palling, D. J., Wustman, B. A., Schiffmann, R., Mahuran, D. J., Lockhart, D. J., and Valenzano, K. J. (2010) The pharmacological chaperone isofagomine increases the activity of the Gaucher disease L444P mutant form of β -glucosidase. *FEBS J.* **277**, 1618–1638
- Liou, B., Kazimierczuk, A., Zhang, M., Scott, C. R., Hegde, R. S., and Grabowski, G. A. (2006) Analyses of variant acid β -glucosidases: effects of

- Gaucher disease mutations. *J. Biol. Chem.* **281**, 4242–4253
23. Dreyfus, H., Guérold, B., Freysz, L., and Hicks, D. (1997) Successive isolation and separation of the major lipid fractions including gangliosides from single biological samples. *Anal. Biochem.* **249**, 67–78
24. Wei, R. R., Hughes, H., Boucher, S., Bird, J. J., Guziewicz, N., Van Patten, S. M., Qiu, H., Pan, C. Q., and Edmunds, T. (2011) X-ray and biochemical analysis of N370S mutant human acid β -glucosidase. *J. Biol. Chem.* **286**, 299–308
25. Xu, Y. H., Ponce, E., Sun, Y., Leonova, T., Bove, K., Witte, D., and Grabowski, G. A. (1996) Turnover and distribution of intravenously administered mannose-terminated human acid β -glucosidase in murine and human tissues. *Pediatr. Res.* **39**, 313–322
26. Sawkar, A. R., Cheng, W. C., Beutler, E., Wong, C. H., Balch, W. E., and Kelly, J. W. (2002) Chemical chaperones increase the cellular activity of N370S β -glucosidase: a therapeutic strategy for Gaucher disease. *Proc. Natl. Acad. Sci. U.S.A.* **99**, 15428–15433
27. Chang, H. H., Asano, N., Ishii, S., Ichikawa, Y., and Fan, J. Q. (2006) Hydrophilic iminosugar active-site-specific chaperones increase residual glucocerebrosidase activity in fibroblasts from Gaucher patients. *FEBS J.* **273**, 4082–4092
28. Sun, Y., Ran, H., Liou, B., Quinn, B., Zamzow, M., Zhang, W., Bielawski, J., Kitatani, K., Setchell, K. D., Hannun, Y. A., and Grabowski, G. A. (2011) Isofagomine *in vivo* effects in a neuropathic Gaucher disease mouse. *PLoS One* **6**, e19037
29. Ishii, S., Chang, H. H., Yoshioka, H., Shimada, T., Mannen, K., Higuchi, Y., Taguchi, A., and Fan, J. Q. (2009) Preclinical efficacy and safety of 1-deoxygalactonojirimycin in mice for Fabry disease. *J. Pharmacol. Exp. Ther.* **328**, 723–731
30. Bülow, A., Plesner, I. W., and Bols, M. (2000) A large difference in the thermodynamics of binding of isofagomine and 1-deoxynojirimycin to β -glucosidase. *J. Am. Chem. Soc.* **122**, 8567–8568
31. Lieberman, R. L., D'aquino, J. A., Ringe, D., and Petsko, G. A. (2009) Effects of pH and iminosugar pharmacological chaperones on lysosomal glycosidase structure and stability. *Biochemistry* **48**, 4816–4827
32. Vaccaro, A. M., Muscillo, M., and Suzuki, K. (1985) Characterization of human glucosylsphingosine glucosyl hydrolase and comparison with glucosylceramidase. *Eur. J. Biochem.* **146**, 315–321
33. Xu, Y. H., Sun, Y., Barnes, S., and Grabowski, G. A. (2010) Comparative therapeutic effects of velaglucerase alfa and imiglucerase in a Gaucher disease mouse model. *PLoS One* **5**, e10750